

Vibrationally resolved photoelectron studies of the $7\sigma^{-1}$ channel in N_2O ^{a)}

T. A. Ferrett, A. C. Parr, S. H. Southworth, and J. E. Hardis

Radiometric Physics Division, National Bureau of Standards, Gaithersburg, Maryland 20899

J. L. Dehmer

Argonne National Laboratory, Argonne, Illinois 60439

(Received 15 September 1988; accepted 28 October 1988)

We present vibrationally resolved photoelectron studies of the 000, 100, 200, and 001 modes of the \tilde{A} state ($7\sigma^{-1}$) of N_2O^+ in the 17.4–26 eV photon-energy range. The vibrational branching ratios $\sigma(100)/\sigma(000)$ and $\sigma(001)/\sigma(000)$ agree very well with fluorescence measurements by Kelly *et al.* and qualitatively with recent theoretical predictions of Braunstein and McKoy. The large non-Franck–Condon variations in the $\sigma(100)/\sigma(000)$ and $\sigma(200)/\sigma(000)$ branching ratios are associated with a predicted $7\sigma \rightarrow \epsilon\sigma$ shape resonance near 20 eV. Overall, the vibrational branching ratios imply lower resonant energies for the stretching modes (100 and 200) and a similar resonant energy for the asymmetric stretch (001), compared with the 000 mode. The vibrational asymmetry parameters (β) display a strong variation with energy which is qualitatively reproduced by theory; however, the experimental values for $\beta(100)$ and $\beta(001)$ exhibit additional structure around 20 eV. When combined with theory and recent fluorescence data, these results help to demonstrate a correlation of shape resonance energy with overall molecular length ($R_{\text{N-N}} + R_{\text{N-O}}$); this important result implies a resonant state which is localized on the entire triatomic molecular frame rather than on the N–N or N–O components.

I. INTRODUCTION

In the photoionization of molecules, quasibound shape resonances occur in the core and valence continua. A shape resonant state results from temporary trapping of the photoelectron by a potential barrier caused by the interplay of centrifugal and electrostatic forces on the perimeter of the molecule.^{1–3} These localized shape resonances correlate well with unoccupied antibonding molecular orbitals familiar in molecular orbital theory.⁴ A great deal of work has been done on diatomics and other small molecules which has helped to elucidate the general properties of this resonance phenomenon.² However, relatively few vibrationally resolved studies have been performed. These vibrational results, including work on CO ,⁵ O_2 ,⁶ and N_2 ,^{7–9} provide an important probe of the dependence of shape resonances on molecular geometry. Excitation into a shape resonance introduces an R dependence into the vibrationally resolved ionization probabilities. For example, theoretical studies of N_2 (Refs. 7 and 9) and CO_2 (Ref. 10) have demonstrated a sensitive dependence of shape resonance energy and width on internuclear separation. Furthermore, it has been proposed that if empirical trends of core-level resonance energies vs bond length could be compiled for many molecules, then it might be possible to deduce bond distances in larger, more complicated systems (adsorbates on surfaces, polymers, ..., etc.).^{11–15} Whether such trends exist depends critically on the degree of localization of shape resonant states between particular nuclei.¹⁶ For these reasons, it is crucial to extend our understanding of shape resonances to polyatomic

molecules, where it is possible to test the response of individual vibrational modes which effectively sample different spatial regions and internuclear distances in the molecule. This detailed information on vibrational dynamics should help to establish the trapping site of the resonant state on the molecular framework, which in polyatomics can inherently take on more complexity than in diatomics.

As one of the important examples, the \tilde{A} ($7\sigma^{-1}$) state of the linear N_2O^+ molecule has been studied experimentally by photoelectron^{17–22} and fluorescence^{23,24} techniques. Earlier results suggested non-Franck–Condon behavior for the vibrational branching ratios especially near the ionization threshold.²³ Until just recently, theoretical work has been done in a vibrationally unresolved manner, revealing two shape resonances in the $7\sigma \rightarrow \epsilon\sigma$ continuum of N_2O at about 20 and 38 eV photon energy.²⁵ The resonance at 38 eV appears only in the experimental asymmetry parameter (β) for the \tilde{A} state, probably because the alternate $7\sigma \rightarrow \epsilon\pi$ continuum dominates the cross section in this energy region. In contrast, the measurable effects are more pronounced at the first resonance just above threshold. New theory results by Braunstein and McKoy illustrate a variety of responses in the measurable parameters (partial cross section, branching ratios, and asymmetry parameters), which are strongly dependent on the vibrational mode, and more specifically, on the overall molecular length of the N_2O^+ molecule.²⁶

We have concentrated our photoelectron study on this first relatively intense shape resonance near 20 eV photon energy for the \tilde{A} (${}^2\Sigma^+$) state of N_2O^+ . This energy range is somewhat complex since autoionizing resonances dominate the photoionization cross section in the first 3 eV above threshold^{22–24,27} (ionization potential = 16.39 eV^{17,27}). We

^{a)} Work supported in part by the U.S. Department of Energy, Office of Health and Environmental Research under Contract No. W-31-109-Eng-38.

have taken a number of spectra through this region and up to 26 eV photon energy, but report here only those results for energies away from or in between the autoionization structure. In this way, we attempt to isolate the dynamics of the vibrational motion due to the shape resonance only. We note that this decoupled view of the shape and autoionizing resonances may be too simplistic, and that some caution must be used in interpreting results. Comparison with new theoretical calculations²⁶ should help to determine the validity of this approach.

We report here vibrational branching ratios for $7\sigma^{-1}$ ionization to the \tilde{A} state of N₂O⁺ for the 100 (symmetric stretch), 001 (asymmetric stretch), and 200 (2 quanta of symmetric stretch) vibrational levels relative to the unexcited 000 level; we compare our data with new fluorescence results of Kelly *et al.*²⁸ In addition, we report the asymmetry parameters for the 000, 100, and 001 levels of the \tilde{A} state, and compare all of our results with Hartree-Fock calculations by Braunstein and McKoy.²⁶

The experimental apparatus is described in Sec. II. Section III includes results and discussion, and conclusions follow in Sec. IV.

II. EXPERIMENTAL

Photoelectron spectra were recorded with two hemispherical electron analyzers (equipped with position-sensitive area detectors) placed at angles $\theta = 0^\circ$ and 90° with respect to the major axis of photon polarization.²⁹ The ionizing radiation in the 10–30 eV range was provided by synchrotron radiation from a 2 m normal-incidence monochromator at the National Bureau of Standard's electron storage ring, the Synchrotron Ultraviolet Radiation Facility (SURF).³⁰ The monochromator bandpass was 0.65(5) Å (0.016 eV at 17.5 eV). The electron analyzers operated at 2 eV pass energy, corresponding to a detector resolution of 15–20 meV. A spectrum taken of the \tilde{A} state of N₂O⁺ at 17.49 eV is shown in Fig. 1, demonstrating a combined resolution of 23 meV in the width of the 000 vibrational level.

Vibrational branching ratios and asymmetry parameters were obtained from peak areas in the photoelectron spectra using the expression for the differential cross section for a randomly oriented sample ionized by elliptically polarized light in the dipole approximation^{29,31}:

$$\frac{d\sigma}{d\Omega} = \frac{\sigma_v(h\nu)}{4\pi} \left[1 + \beta_v \frac{(h\nu)}{4} (3P \cos 2\theta + 1) \right], \quad (1)$$

where P is the polarization of the photon beam, θ is the angle between the major photon polarization axis and the electron emission direction, and $\sigma_v(h\nu)$ and $\beta_v(h\nu)$ are the partial cross section and asymmetry parameter for the vibrational level v at the photon energy $h\nu$. In practice, we can reliably determine ratios of peaks in spectra taken simultaneously at $\theta = 0^\circ$ and 90° , and thus report vibrational branching ratios and β 's. In this study, we report branching ratios relative to the unexcited 000 level of the \tilde{A} state, i.e., $\sigma(100)/\sigma(000)$.

The transmission and relative efficiency of the electron detectors were calibrated with Ar $3p$ photoionization, for which the cross section and β are known.³² The polarization

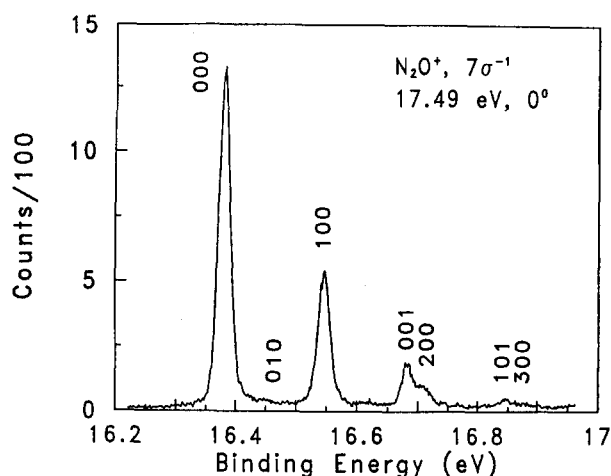


FIG. 1. Photoelectron spectrum of the \tilde{A} ($7\sigma^{-1}$) state of N₂O⁺ taken at 17.49 eV photon energy and $\theta = 0^\circ$ with respect to the major axis of the photon polarization. Vibrational components are labeled.

of the light beam was determined to be 0.67(2) using a triple-reflection device³³ and was checked by measuring the angular distribution of He $1s$ photoelectrons for which $\beta = 2.0$. The spectra were fit with a nonlinear least squares method using Gaussian line shapes to extract peak areas.

III. RESULTS AND DISCUSSION

Results for the vibrational branching ratios and β 's are included in Tables I and II, respectively. We discuss first the

TABLE I: Vibrational branching ratios for photoionization of the \tilde{A} state of N₂O⁺ as a function of photon energy. Uncertainties are given in parentheses.

$h\nu$ (eV)	100/000	001/000	200/000	200/100
17.38	0.429(10)	0.103(4)	0.0533(34)	0.124(9)
17.42	0.433(14)	0.102(5)	0.0570(55)	0.132(13)
17.45	0.414(14)	0.097(5)	0.0509(49)	0.123(13)
17.49	0.416(13)	0.107(6)	0.0512(54)	0.123(10)
18.39	0.316(9)	0.086(5)	0.0219(34)	0.069(11)
18.70	0.300(9)	0.084(5)	0.0288(43)	0.096(15)
19.32	0.253(6)	0.080(4)	0.0170(26)	0.067(10)
19.53	0.223(6)	0.084(5)	0.0134(29)	0.060(13)
19.82	0.223(5)	0.088(4)	0.0158(19)	0.071(9)
19.98	0.213(6)	0.086(5)	0.0120(24)	0.057(11)
20.23	0.210(6)	0.076(4)	0.0063(15)	0.030(7)
20.48	0.209(5)	0.075(3)	0.0069(12)	0.033(6)
20.73	0.209(7)	0.081(5)	0.0077(19)	0.037(9)
20.98	0.209(5)	0.092(4)	0.0083(14)	0.040(7)
21.23	0.213(7)	0.091(5)	0.0096(25)	0.045(12)
21.48	0.219(7)	0.094(5)	0.0071(17)	0.033(8)
21.73	0.223(8)	0.095(5)	0.0059(20)	0.026(9)
21.98	0.224(6)	0.095(4)	0.0081(15)	0.036(7)
22.23	0.221(8)	0.097(4)	0.0086(21)	0.039(9)
22.48	0.221(9)	0.103(6)	0.0064(21)	0.029(10)
22.73	0.222(9)	0.104(6)	0.0083(18)	0.037(8)
22.98	0.225(10)	0.111(7)	0.0081(23)	0.036(10)
23.23	0.223(10)	0.109(6)	0.0071(18)	0.032(8)
23.48	0.229(10)	0.111(6)	0.0110(21)	0.048(9)
23.98	0.246(11)	0.107(7)	0.0125(27)	0.051(11)
24.48	0.250(12)	0.110(8)	0.0144(46)	0.058(19)
24.98	0.251(11)	0.110(8)	0.0119(33)	0.047(13)
25.48	0.255(7)	0.113(6)	0.0176(22)	0.069(9)
25.98	0.272(13)	0.115(9)	0.0196(53)	0.072(20)

TABLE II: Vibrationally resolved asymmetry parameters (β) for photoionization to the \tilde{A} state of N₂O⁺. Uncertainties are given in parentheses.

$h\nu$ (eV)	$\beta(000)$	$\beta(100)$	$\beta(001)$
17.38	-0.314(11)	-0.267(12)	0.028(25)
17.42	-0.302(15)	-0.276(17)	-0.023(35)
17.45	-0.329(16)	-0.265(17)	0.027(35)
17.49	-0.290(10)	-0.252(10)	-0.014(25)
18.39	-0.250(13)	-0.159(16)	0.086(38)
18.70	-0.237(13)	-0.182(18)	0.118(41)
19.32	-0.122(10)	0.115(19)	0.297(45)
19.53	0.033(10)	0.371(30)	0.274(46)
19.82	0.049(8)	0.411(28)	0.432(43)
19.98	0.169(12)	0.621(40)	0.717(59)
20.23	0.246(15)	0.629(40)	0.781(64)
20.48	0.304(13)	0.697(32)	0.875(50)
20.73	0.362(20)	0.670(41)	0.885(69)
20.98	0.389(15)	0.697(31)	0.777(45)
21.23	0.430(23)	0.686(42)	0.749(59)
21.48	0.466(25)	0.641(40)	0.768(61)
21.73	0.527(28)	0.670(41)	0.766(58)
21.98	0.559(21)	0.681(35)	0.805(44)
22.23	0.596(32)	0.706(43)	0.731(56)
22.48	0.605(33)	0.764(49)	0.785(64)
22.73	0.666(36)	0.813(49)	0.813(59)
22.98	0.723(39)	0.841(51)	0.840(62)
23.23	0.784(43)	0.901(54)	0.848(60)
23.48	0.774(42)	0.914(54)	0.812(58)
23.98	0.844(47)	0.888(54)	0.916(69)
24.48	0.906(51)	0.843(52)	0.947(74)
24.98	0.885(50)	0.792(50)	0.894(73)
25.48	0.884(35)	0.943(40)	0.789(47)
25.98	0.945(53)	0.827(52)	0.785(69)

behavior of the branching ratios in Sec. III A and the β 's in Sec. III B.

A. Branching ratios

The vibrational branching ratios relative to the 000 level provide a way to compare the behavior of the various vibrational channels near the first shape resonance for the \tilde{A} state of N₂O⁺. In Fig. 2 the 100 and 001 branching ratios are plotted with fluorescence results of Kelly *et al.*²⁸ (which have been scaled to our absolute branching ratios) and theo-

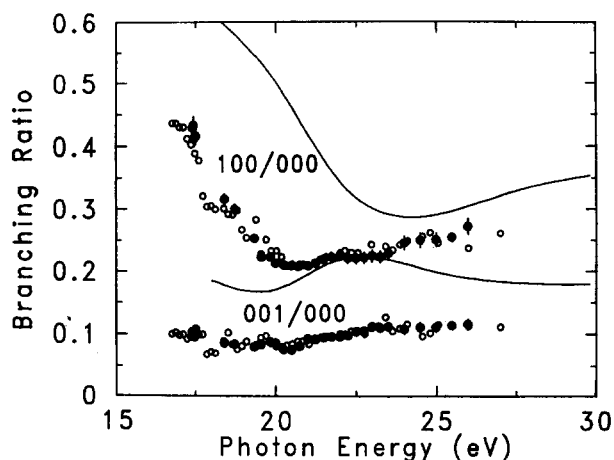


FIG. 2. Branching ratio data for the 100 and 001 vibrational levels of the \tilde{A} ($7\sigma^{-1}$) state of N₂O⁺ relative to the 000 level. Filled circles are our data; open circles are from Kelly *et al.* (Ref. 28); theory curves from Braunstein and McKoy (Ref. 26).

ry results of Braunstein and McKoy.²⁶ Our results are in excellent agreement with fluorescence measurements, and all the experimental data display the qualitative features which appear in theory. Since the theory includes only one-electron effects, the qualitative agreement is an indication that the branching-ratio curves are governed mainly by the predicted $7\sigma \rightarrow \epsilon\sigma$ shape resonance. There is a shift of about 2 eV to higher energy for the shape resonance in the theoretical results, which is also evident when the relative partial cross sections from fluorescence²⁸ are compared to theory. The theoretical branching-ratio curves are higher than experiment, probably caused by uncertainties in the molecular potentials and modeling of the vibrational wave functions.²⁶ For a more extensive discussion of the approximations made in the theory, we refer the reader to the accompanying paper by Braunstein and McKoy.²⁶

The most striking result is the strong non-Franck-Condon variation in the 100 branching ratio near the shape resonance (17–20 eV, see Fig. 2). The steep rise toward threshold does not appear to be directly related to the autoionizing structure present below 20 eV. Our spectra were taken away from these resonances, as were those of Kelly *et al.*²⁸ Earlier studies^{22–24} investigated the sharper resonant structure in more detail, and found it superimposed on a nonconstant branching ratio which increased toward threshold.²³

This rise is a direct indication that the 100 and 000 vibrational channels exhibit different resonance energies and widths in the partial cross sections. In fact, fluorescence measurements see these differences directly: the 100 cross section peaks to lower photon energy and displays a narrower profile than does the 000 mode.²⁸

In contrast, the 001 branching ratio appears nearly flat over the entire photon-energy range covered in this study. This indicates that the 000 and 001 partial cross sections peak at nearly the same energy and have nearly the same width.

We have extended our vibrational investigation of the \tilde{A} state of N₂O⁺ to the 200 level which is partially resolved in our spectrum (see Fig. 1) and has not been studied by fluorescence techniques. In Fig. 3, we show the $\sigma(200)/\sigma(000)$ branching ratio (top), which increases strongly near threshold, as did the $\sigma(100)/\sigma(000)$ branching ratio. Preliminary calculations by Braunstein qualitatively suggest the same trend.³⁴ As with the 100 branching ratio, this implies a cross section which is peaked at lower energy and is likely narrower in width than that for the 000 level. We note that the relative increase toward threshold is even larger for the 200 branching ratio than that for the 100 branching ratio; this implies stronger non-Franck-Condon behavior in weaker vibrational components, as was observed in diatomics.⁷

We gain even more information by plotting the $\sigma(200)/\sigma(100)$ branching ratio in Fig. 3 (bottom), allowing us to compare the behavior of one and two quanta of symmetric stretch. There is indeed an increase in this branching ratio, confirming a shift to lower resonance energy for the 200 mode relative to the 100 mode.

To summarize, compared with the 000 vibrational channel, the stretching modes (100 and 200) exhibit strong

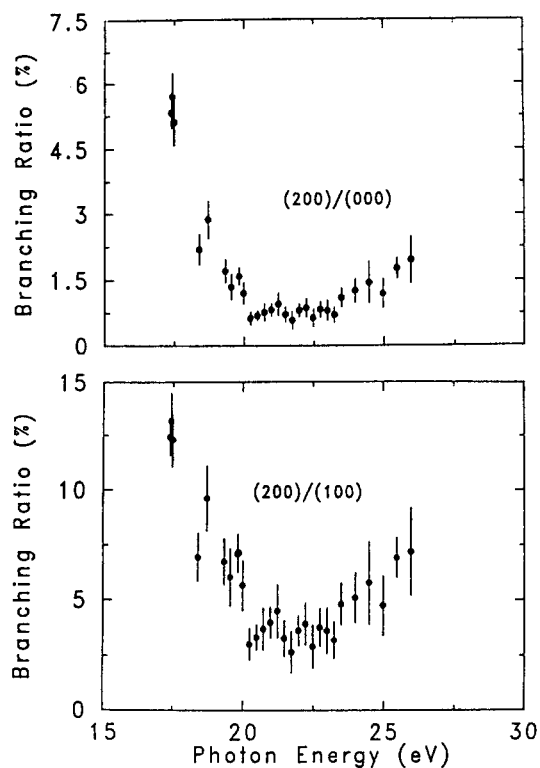


FIG. 3. Top: Branching ratio for the 200 level relative to the 000 level for $7\sigma^{-1}$ ionization of N_2O . Bottom: Branching ratio for the 200 level relative to the 100 level for $7\sigma^{-1}$ ionization of N_2O .

non-Franck-Condon behavior (and shifts in resonance energy) in the vicinity of the σ shape resonance near 20 eV; the asymmetric stretch (001) does not. The overall molecular length for the 001 and 000 modes are quite similar, since the compensating motion of the asymmetric stretch tends to preserve molecular length. In contrast, the stretching modes involve significant changes in molecular length. As a whole then, the vibrational results seem to show a correlation of shape-resonance energy with overall molecular length ($R_{N-N} + R_{N-O}$). This trend has been revealed to a greater extent by theoretical calculations by Braunstein and McKoy²⁶ which examined how changes in individual bond lengths and overall molecular length affected the shape resonance positions. This study found that the shape resonance energy varied as $1/l^2$ (where l is the overall molecular length) in N_2O near the 20-eV feature,²⁶ in contrast to more simple expectations of a correlation with a single bond distance (either N-N or N-O). Thus, it is likely that the resonant state is localized on the entire molecular frame (not simply between the N-N or N-O atoms). With this result, N_2O becomes an important example of polyatomic shape-resonant behavior. Using the vibrational motion as a probe of internuclear distance provides qualitative information on the nature of the trapping site of the resonant state in a polyatomic molecule. In this case, there is a more complex spatial character to the continuum wave function than is possible with diatomics.

B. Asymmetry parameters

In Fig. 4 we present the 100 and 001 vibrational β 's compared with $\beta(000)$ and with theory results of Braun-

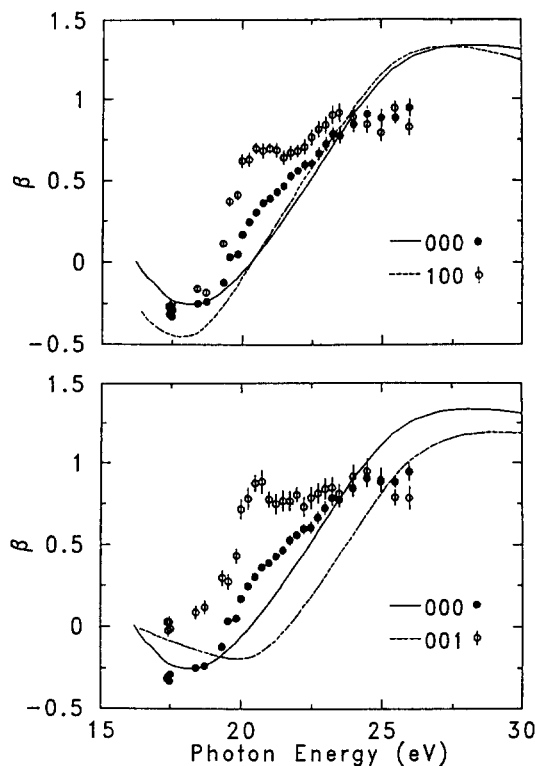


FIG. 4. Top: Asymmetry parameters for the 100 (open circles) and 000 (filled circles) vibrational components of the \bar{A} state of N_2O^+ . Theory results from Braunstein *et al.* (Ref. 26) are shown for the 000 (solid) and 100 (dashed) levels, shifted 2 eV to lower energy for comparison. Bottom: Asymmetry parameters for the 001 (open circles) and 000 (filled circles) vibrational components of the A state of N_2O^+ . Theory results from Braunstein *et al.* (Ref. 26) are shown for the 000 (solid) and 001 (dashed) levels, shifted 2 eV to lower energy for comparison.

stein and McKoy.²⁶ The theory curves have been shifted 2 eV to lower energy for purposes of comparison. The theory results²⁶ show different minimum values of β close to threshold for each vibrational level, with the $\beta(001)$ minimum shifted several eV to higher energy than the others. Our data are generally consistent with a minimum near threshold, followed by a rise to higher energy, with the exception of the additional oscillations in $\beta(100)$ and $\beta(001)$ at about 20 eV. The approximate width of this additional feature is 2 eV. These oscillations appear as a "spreading" of the β 's (100 and 001 vs 000) with a maximum separation near 20.5 eV photon energy. Early data of Carlson *et al.*²¹ qualitatively display the same effect when care is taken to exclude those values on autoionizing resonances. This spreading effect does not appear in the theory curves.²⁶ In fact, $\beta(001)$ is predicted to be less than $\beta(000)$ in the range $h\nu = 20$ –25 eV; the opposite is true of the experimental values.

In general, v -dependent β 's are the counterpart to non-Franck-Condon vibrational intensities resulting from shape resonance behavior.⁷ Therefore, the v -dependence in the experimental β 's near 20 eV, including the oscillations in $\beta(100)$ and $\beta(001)$, may reflect the action of the σ shape resonance. However, the discrepancies between theory and experiment for the β 's near 20 eV are puzzling in view of the success of Hartree-Fock calculations in modeling the one-electron behavior of photoionization in N_2 .⁹ For N_2O , the

quality of the theory²⁶ and the vibrational wave functions is clearly adequate to reproduce qualitatively the experimental branching ratios and to extract the essential physical result of the relation between the overall molecular length and resonance energy. The more subtle effects in our experimental β curves may require improvement in the vibrational wave functions, which are difficult to model because of uncertainties in the N₂O⁺ molecular potentials. However, it may be necessary to consider other effects such as autoionization (which is clearly pertinent between 17 and 20 eV and possibly at higher energies for doubly excited states) and continuum-continuum coupling.

IV. CONCLUSIONS

We have reported results for photoionization to the \tilde{A} state of N₂O⁺ and its associated vibrational levels: 000, 100, 200, and 001. With the aid of recent theory by Braunstein and McKoy,²⁶ there is a good evidence that the non-Franck-Condon oscillations in the vibrational branching ratios are related primarily to the $7\sigma \rightarrow \epsilon\sigma$ shape resonance. However, there are discrepancies between theory and experiment for the vibrationally resolved β parameters. It is essential to resolve these discrepancies and identify whether there is a problem in the presently developed Hartree-Fock modeling of shape resonances in polyatomics (uncertainties in molecular potentials have already been identified), or whether more complicated multielectron effects are responsible for the observed β oscillations.

Experimentally, studies which examine other molecules, particularly in bending and combination modes, may provide even more information on how vibrational motion is affected by the spatial characteristics of shape resonant states. Complementary core-level studies, such as the recent work on the N and O 1s levels of N₂O,³⁵ have the ability to selectively excite from a highly localized site to help determine the characteristics of shape resonances, which may vary from core to valence orbitals.

More generally, this vibrationally resolved photoelectron study on N₂O has extended our knowledge of the vibrational dynamics of shape resonances in polyatomic molecules. Our branching ratios (particularly for the 200 level) and β 's provide additional information which is complementary to recent fluorescence results.²⁸ Both experimental studies, when combined with recent theoretical calculations,²⁶ illustrate that polyatomics may exhibit localized shape resonant states which extend spatially over more than one bond. Thus, caution must be exercised when associating shape resonances in polyatomics with particular bonds; the validity of a one-to-one correspondence should be determined on a case-by-case basis. This important result highlights the utility of vibrationally resolved measurements as a probe of internuclear distance to elucidate the basic aspects of resonance phenomena.

ACKNOWLEDGMENTS

We gratefully acknowledge the staff of SURF at the National Bureau of Standards for assistance and cooperation during the experimental measurements. We thank M.

Braunstein, V. McKoy, E. Poliakoff, and L. Kelly for helpful discussions and for providing us with results prior to publication. Work was supported in part by the U.S. Department of Energy, Office of Health and Environmental Research under Contract No. W-31-109-Eng-38.

- ¹J. L. Dehmer, *J. Chem. Phys.* **56**, 4496 (1972).
- ²J. L. Dehmer, A. C. Parr, and S. H. Southworth, in *Handbook on Synchrotron Radiation, Vol. II*, edited by G. V. Marr (North-Holland, Amsterdam, 1986); J. L. Dehmer, in *Resonances in Electron-Molecule Scattering, van der Waals Complexes, and Reactive Chemical Dynamics*, edited by D. G. Truhlar (American Chemical Society, Washington, D.C., 1984); J. L. Dehmer, D. Dill, and A. C. Parr, in *Photophysics and Photochemistry in the Vacuum Ultraviolet*, edited by S. P. McGlynn, G. Findley, and R. Huebner (Reidel, Dordrecht, 1985).
- ³D. L. Lynch, V. McKoy, and R. R. Lucchese, in *Resonances in Electron-Molecule Scattering, van der Waals Complexes, and Reactive Chemical Dynamics*, edited by D. G. Truhlar (American Chemical Society, Washington, D.C., 1984).
- ⁴P. W. Langhoff, in Ref. 3.
- ⁵R. Stockbauer, B. E. Cole, D. L. Ederer, J. B. West, A. C. Parr, and J. L. Dehmer, *Phys. Rev. Lett.* **43**, 757 (1979); B. E. Cole, D. L. Ederer, R. Stockbauer, K. Codling, A. C. Parr, J. B. West, E. Poliakoff, and J. L. Dehmer, *J. Chem. Phys.* **72**, 6308 (1980); N. Padiyal, G. Csanak, B. V. McKoy, and P. W. Langhoff, *ibid.* **69**, 2992 (1978).
- ⁶G. Raseev, H. Lefebvre-Brion, H. Le Rouzo, and A. L. Roche, *J. Chem. Phys.* **74**, 6686 (1981); P. M. Morin, I. Nenner, M. Y. Adam, H. J. Hubin-Franskin, and J. Delwiche, *Chem. Phys. Lett.* **92**, 609 (1982).
- ⁷J. L. Dehmer, D. Dill, and S. Wallace, *Phys. Rev. Lett.* **43**, 1005 (1979).
- ⁸J. B. West, A. C. Parr, B. E. Cole, D. L. Ederer, R. Stockbauer, and J. L. Dehmer, *J. Phys. B* **13**, L105 (1980).
- ⁹R. R. Lucchese and V. McKoy, *J. Phys. B* **14**, L629 (1981); T. A. Carlson, M. O. Krause, D. Mehaffy, J. W. Taylor, F. A. Grimm, and J. D. Allen, Jr., *J. Chem. Phys.* **73**, 6056 (1980).
- ¹⁰J. R. Swanson, D. Dill, and J. L. Dehmer, *J. Phys. B* **14**, L207 (1981).
- ¹¹J. Stöhr, J. L. Gland, W. Eberhardt, D. Outka, R. J. Madix, F. Sette, R. J. Koestner, and U. Doebler, *Phys. Rev. Lett.* **51**, 2414 (1983).
- ¹²A. P. Hitchcock, S. Beaulieu, T. Steel, J. Stöhr, and F. Sette, *J. Chem. Phys.* **80**, 3927 (1984).
- ¹³J. Stöhr, F. Sette, and A. L. Johnson, *Phys. Rev. Lett.* **53**, 1684 (1984).
- ¹⁴F. Sette, J. Stöhr, and A. P. Hitchcock, *J. Chem. Phys.* **81**, 4906 (1984); *Chem. Phys. Lett.* **110**, 517 (1984).
- ¹⁵F. Sette, J. Stöhr, E. B. Kollin, D. J. Dwyer, J. L. Gland, J. L. Robbins, and A. L. Johnson, *Phys. Rev. Lett.* **54**, 935 (1985).
- ¹⁶M. N. Piancastelli, D. W. Lindle, T. A. Ferrett, and D. A. Shirley, *J. Chem. Phys.* **86**, 2765 (1987).
- ¹⁷C. R. Brundle and D. W. Turner, *Int. J. Mass Spectrom. Ion Phys.* **2**, 195 (1969).
- ¹⁸R. Frey, B. Gotchev, W. B. Peatman, H. Pollak, and E. W. Schlag, *Chem. Phys. Lett.* **54**, 411 (1978).
- ¹⁹P. M. Dehmer, J. L. Dehmer, and W. A. Chupka, *J. Chem. Phys.* **73**, 126 (1980).
- ²⁰C. M. Truesdale, S. Southworth, P. H. Kobrin, D. W. Lindle, and D. A. Shirley, *J. Chem. Phys.* **78**, 7117 (1983).
- ²¹T. A. Carlson, P. R. Keller, J. W. Taylor, T. Whitley, and F. A. Grimm, *J. Chem. Phys.* **79**, 97 (1983).
- ²²T. A. Carlson, W. A. Svensson, and M. O. Krause, *J. Chem. Phys.* **83**, 3738 (1985).
- ²³E. D. Poliakoff, M.-H. Ho, M. G. White, and G. E. Leroi, *Chem. Phys. Lett.* **130**, 91 (1986).
- ²⁴E. D. Poliakoff, M.-H. Ho, G. E. Leroi, and M. G. White, *J. Chem. Phys.* **85**, 5529 (1986).
- ²⁵M. Braunstein and V. McKoy, *J. Chem. Phys.* **87**, 224 (1987).
- ²⁶M. Braunstein and V. McKoy, *J. Chem. Phys.* **90**, 1535 (1989).
- ²⁷J. Berkowitz and J. H. D. Eland, *J. Chem. Phys.* **67**, 2740 (1977).
- ²⁸L. A. Kelly, L. M. Duffy, B. Space, E. D. Poliakoff, P. Roy, S. H. South-

- worth, and M. G. White, *J. Chem. Phys.* **90**, 1544 (1989).
- ²⁹A. C. Parr, S. H. Southworth, J. L. Dehmer, and D. M. P. Holland, *Nucl. Instr. Methods* **208**, 767 (1983); **222**, 221 (1984).
- ³⁰D. L. Ederer, B. E. Cole, and J. B. West, *Nucl. Instrum. Methods* **172**, 185 (1980).
- ³¹J. A. R. Samson and A. F. Starace, *J. Phys. B* **8**, 1806 (1975); *Corrigendum* **12**, 3993 (1979).
- ³²G. V. Marr and J. B. West, *At. Data Nucl. Data Tables* **18**, 497 (1976); J. A. R. Samson (private communication); S. H. Southworth, A. C. Parr, J. E. Hardis, J. L. Dehmer, and D. M. P. Holland, *Nucl. Instrum. Methods* **246**, 782 (1986).
- ³³See, for example, V. G. Horton, E. T. Arakawa, R. N. Hamm, and M. W. Williams, *Appl. Optics* **8**, 667 (1969).
- ³⁴M. Braunstein (private communication).
- ³⁵F. A. Grimm, T. A. Carlson, J. Jimenez-Mier, B. Yates, J. W. Taylor, and B. P. Pullen, *J. Electron Spectrosc.* **47**, 257 (1988).